AIMS Geosciences

AIMS Geosciences, 5(2): 145–162.
DOI: 10.3934/geosci.2019.2.145
Received: 15 February 2019
Accepted: 28 April 2019
Published: 15 May 2019

http://www.aimspress.com/journal/geosciences

Research article

Characterization of the Blessington sand geotechnical test site

David Igoe[1],* and Kenneth Gavin[2]

[1] Assistant Professor, Department of Civil, Structural and Environmental Engineering, University of Dublin, Trinity College, Dublin 2, Ireland
[2] Professor of Subsurface Engineering, Geo-Engineering Section, Faculty of Civil Engineering and Geosciences, Delft University of Technology, Netherlands

* **Correspondence:** Eamil: igoed@tcd.ie; Tel: +353018963805.

Abstract: The paper describes the site characterization of a dense sand test site developed by the authors in an active quarry located near the village of Blessington, Ireland. The site has been used to investigate the field response of a number of foundation systems including jacked closed and open-ended piles, driven concrete and steel open-ended piles, shallow footings, bored axially loaded piles and laterally loaded steel piles. The soil at the location is an over-consolidated, glacially deposited, dense to very dense fine sand with a CPT q_c resistance, that increases from ≈10 MPa near the ground surface to 15–20 MPa over a depth of 10 m. The paper describes the geological history of the deposit, composition and mineralogy analyzed through Scanning Electron Microscopy. The results of in-situ tests including CPT, DMT and MASW are presented. Material properties including strength and stiffness derived from laboratory tests are compared to correlation made with in-situ testing. The results of previously unpublished laboratory interface shear box tests to investigate pile ageing effects are presented.

Keywords: sand; pile testing; ageing; CPT

1. Introduction

Since 2001, the Blessington Redbog quarry has been used as a test bed for geotechnical researchers at University College Dublin (UCD), Trinity College Dublin (TCD), Cork Institute of Technology (CIT) and Delft University of Technology (TUD). The area was developed by the authors as part of a number of PhD and post-doctoral research projects which investigated different aspects of foundation behaviour including axial pile behaviour, lateral pile resistance, cyclic loading

response and pile ageing [1–8]. This test site was selected because the strength and stiffness properties of the dense sand (derived from CPT) were highly consistent across the site and deemed to be broadly similar to those encountered in offshore seabed deposits in the North Sea [9].

2. Test sites and location

The test sites are located in the Roadstone Redbog quarry, located approximately 25 km south-west of Dublin. The testing area is approximately 1km to the north-west of Blessington village (Figure 1a), and is divided into two sites, the upper-site which is a 30 m × 30 m area near the entrance to the Redbog quarry, and a lower-site which is approx. 30 m × 60 m. The lower-site is adjacent the upper-site (Figure 1b) but is at approximately 15 m lower elevation as a result of previous quarrying. All testing prior to 2015 was undertaken at the upper-site. Due to space restrictions, the majority of testing since 2015 has been undertaken at the lower-site (Figure 2). The upper site is partially saturated and the water table was identified approximately 2.5 m below ground level at the lower site.

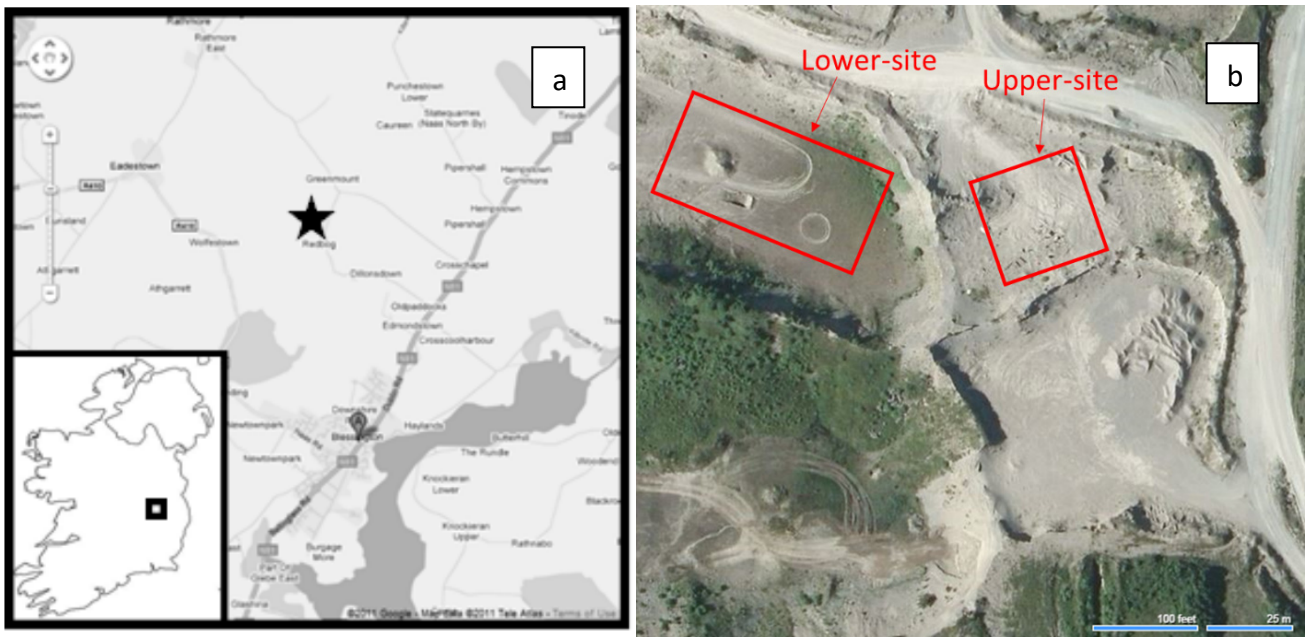

Figure 1. a) Redbog quarry location (after [9]) and b) aerial image of Blessington test sites.

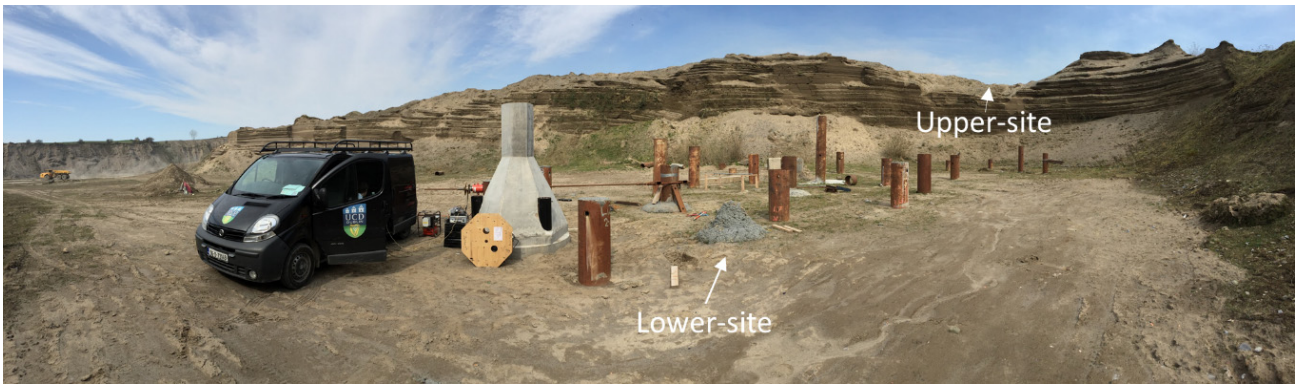

Figure 2. Photograph from Blessington lower-site.

3. Geology

The development of the complex ice contacted delta sequences evident in the area have been studied by numerous researchers [10–12]. The available data and results of many years investigation of the area are synthesised by Philcox [13] who provides an interpretation of the evolution of the delta complex. The sediments of the Blessington sand and gravel pits represent the deposits of a lacustrine delta complex (where sediment carried by a river is deposited as the water slows down as it flows into a lake), with the glacial lake being impounded by the Midlandian ice sheet to the west and by the Wicklow Mountains to the east. The sediments, locally underlain by slates and shale of Silurian age, have a maximum thickness of 60 m, but the exact age of these deposits is uncertain [14]. There are two main phases of deposition, the earlier stage is linked to the retreat of the ice sheet around 20–24 ka (kiloannum) and a later ice re-advance dated at 17 ka [14].

The complex is comprised of a frequently contorted sequence of dominantly gravelly to coarse- to medium-grained sand beds and facies associated with a typical Gilbert-type delta (a specific type of delta characterised by predominantly coarse sediments). However, the test sites in question are relatively well sorted, fine- to medium-grained sand facies [3]. The sediments at the test site correspond to the Light Brown Unit, described by [8], and form the uppermost part of a significant local fluvial channel system. The sand deposits comprise of horizontal, interlaminated (5–15 cm scale), rippled cross-laminated sands and silts, which are typical of low energy fluvial current deposit. A later, but limited, ice re-advance (associated with the 17 ka event) was likely to have covered the study area, the final retreat of which resulted in the deposition of a minimum of 7 m overburden depth above the upper-site area (~22 m above the lower-site). The sites were potentially buried under significantly more than the observed 7 m, and this additional sedimentation may have been removed by erosion during the Holocene (last 12 ka). Unquantified post-glacial isostatic rebound during this period means that it is difficult to constrain the thickness of any sediment removed, but there is certainly sufficient potential overburden (ice and/or sediment) to account for the over-consolidation noted at both test sites [3].

4. Particle size distribution

Kirwan [15] performed Particle Size Distribution sieve tests on samples from cores removed from the upper-site using the sonic coring technique. Nine depths below ground level (between 1.75 m and 11.9 m) were analyzed. On average, the tests showed a soil made up of 92% sand and 8% fines (defined as particles smaller than 0.06 mm). Figure 3 shows the particle size distribution (PSD) curves for each sample depth. Analysis of the PSD graphs gave values of the particle size properties D_{60}, D_{10} and the uniformity coefficient, UC (defined as D_{60}/D_{10}). Figure 4 shows the variation in fines content, D_{60}, D_{10} and UC with depth. The percentage of fines varies from 4% to 13% with a mean value of 8.3%. The mean value of D_{60} was 0.21 mm and D_{10} was 0.093 mm. A mean uniformity coefficient of 2.4 was calculated. The sand is classified as silty, fine to medium SAND based on the results of these sieve tests [9].

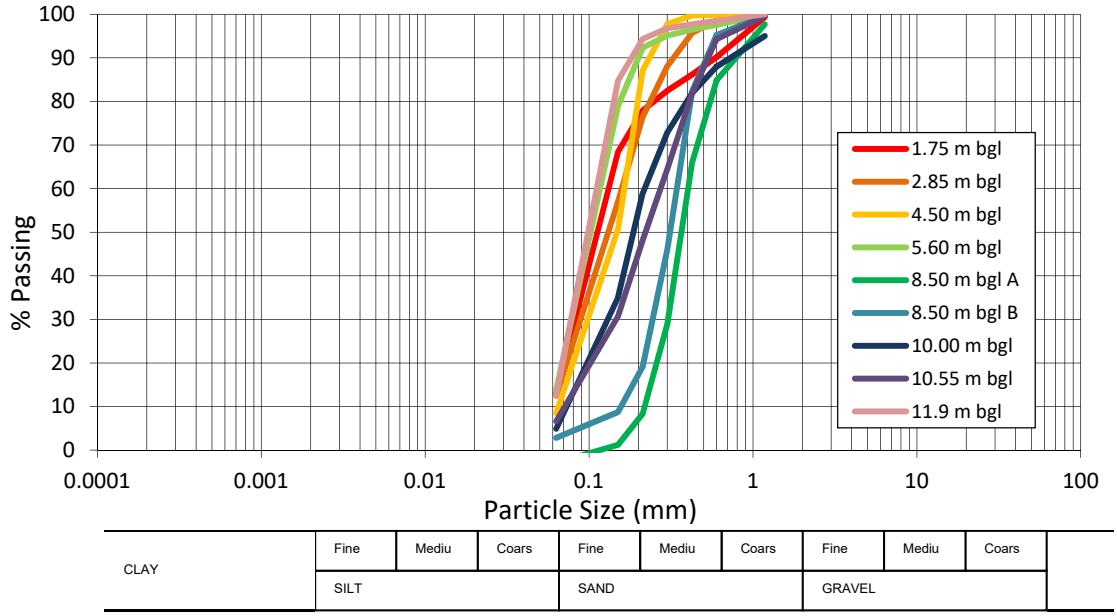

Figure 3. Particle Size Distributions from Blessington upper-site (after [9]).

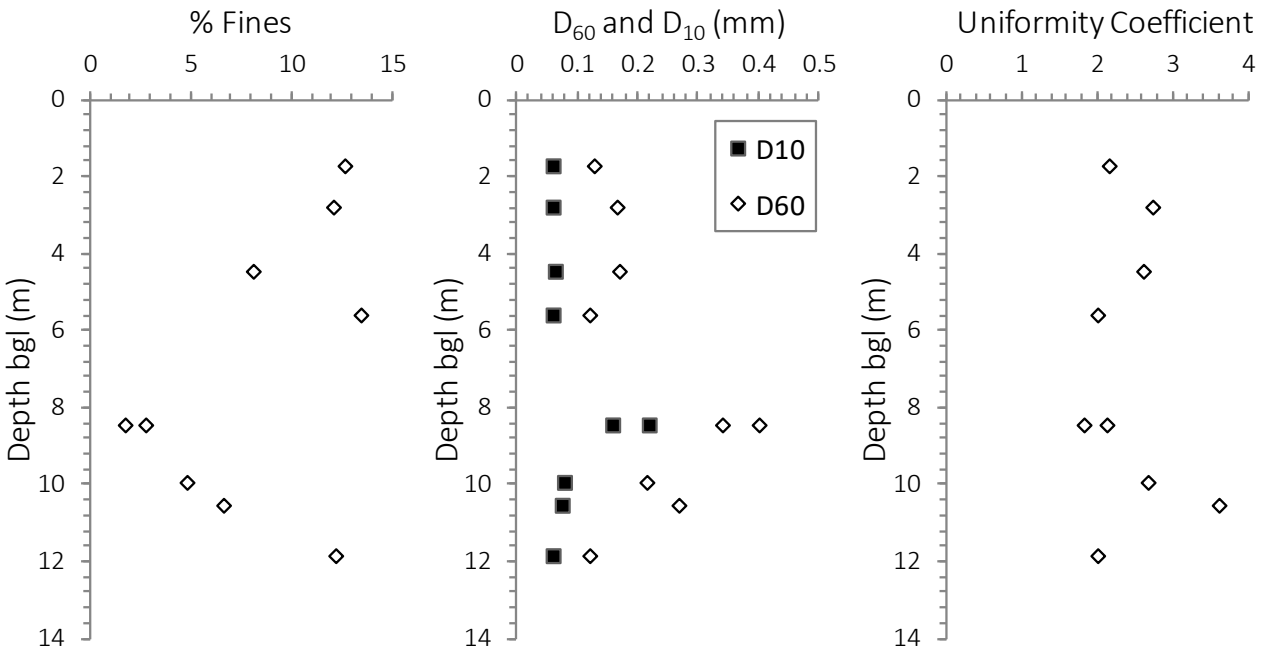

Figure 4. Results of PSD analysis from Blessington upper-site.

5. Particle mineralogy

The particle mineralogy for the Blessington upper-site was investigated firstly using petrographic analysis and secondly using analysis of Scanning Electron Microscopy (SEM) X-ray Diffraction Patters (EDS). Samples for analyses were prepared from cores removed from the upper-site using the sonic coring technique at depths of 1.75 m, 4.5 m, 7.7 m and 11.9 m below ground level. The analyses are described in the following sections.

5.1. Petrographic analysis

Optical petrography performed on the samples shows the sand fraction is dominated by fragments of quartz. The sands also comprise a significant calcite component, both as fragments of spar and as fine-grained micritic mud (presumably derived from nearby limestone bedrock). Subordinate minerals present include feldspar and minor muscovite mica—consistent with derivation from a granitic source. A matrix of clay mineral pervades the interstices and coats the framework grains (Figure 5). The shallowest sample (1.75 m) had the highest clay content with deeper samples showing less clay minerals. This apparent correlation between clay content and depth is unlikely to be consistent throughout the whole section. Rather, the clay content is likely to vary on a smaller scale than the sampling interval, reflecting the laminated nature of the section and transitions between medium and fine-grained sediments [9].

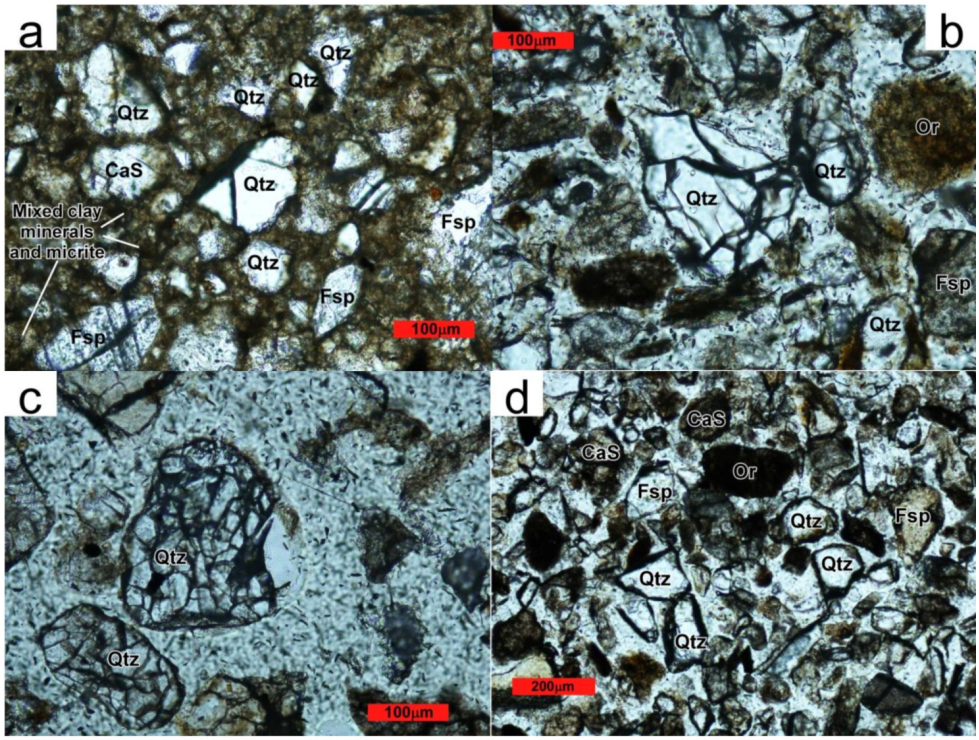

Figure 5. Photomicrographs, in Plane Polarized Light, of Samples from; (a) 1.75 m (b) 4.5 m (c) 7.7 m (d) 11.9 m (after [9]).

5.2. Scanning electron microscopy X-ray diffraction patterns

Particle mineralogy was also determined using an energy-dispersive X-ray spectrometer (EDS) called SwiftED-TM, which was connected to the SEM. Analysis of each SEM EDS spectrum was carried out and compared to the standard spectrum of each mineral likely to be found in the soil samples based on the preliminary petrographic analysis—namely quartz, calcite, feldspar and kaolinite. A number of spectra were taken at each sampling level and the corresponding minerals were noted for each spectrum. The overall results from this analysis are shown in Figure 6. As can be seen from the above figure, quartz dominates the soil's make-up, with a small scattering of calcite, iron and kaolinite. Several spectra were very unusual and a mineral could not be assigned to them, hence the "unknown" bar. This analysis is in strong agreement with the petrographic analysis discussed previously.

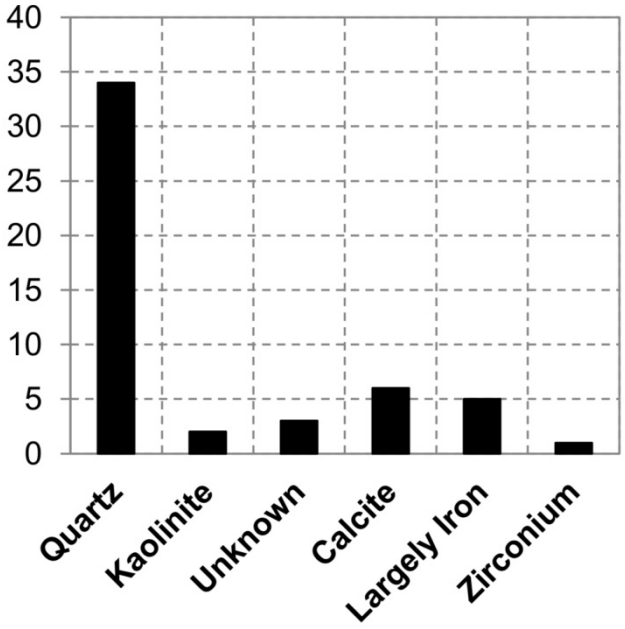

Figure 6. Minerals Found in Borehole Soil Samples from SEM EDS Spectra (after [9]).

6. Particle morphology

Two methods were used to determine the soil's typical morphology. The first method was simple visual observation of scanning electron microscope (SEM) images taken of soil samples from the sonic core borehole. The second method uses calculations on various measurements taken of specific particles to work out morphology parameters such as roundness and angularity. The observed samples showed a mixture of larger particles surrounded by smaller particles, with the proportion of fine particles varying with depth. The large particles appear to be highly fractured (Figure 7), however, the edges of the particles are still sharp rather than rounded (Figure 7d). At smaller scales, the particles tended to appear similar to larger particles suggesting that they are particles of rock flour that had broken away from larger (parent) particles [9]. However, some samples contained plate-like particles of clay minerals, which were shown to be Kaolinite (Figure 7e). For the most part, the sand grains

were consistent with clean quartz sand as observed by the conchoidal fracture patterns (Figure 7f). This mineralogy was confirmed using X-ray diffraction (energy-dispersive X-ray spectrometer-EDS) analysis. Highly angular and fractured particles were observed at all depths. The only difference in depth-dependent variation was the quantity of fines in the sample. This was apparent from macroscale observations from the site, where depositional lenses are present. This observation was also visible in the petrographic analysis. The variation in fines content can be attributed to the mechanism by which the deposit formed—i.e. a glacial delta complex. During periods of high flow rates, fewer fines were deposited to the lake bed, and vice versa [9].

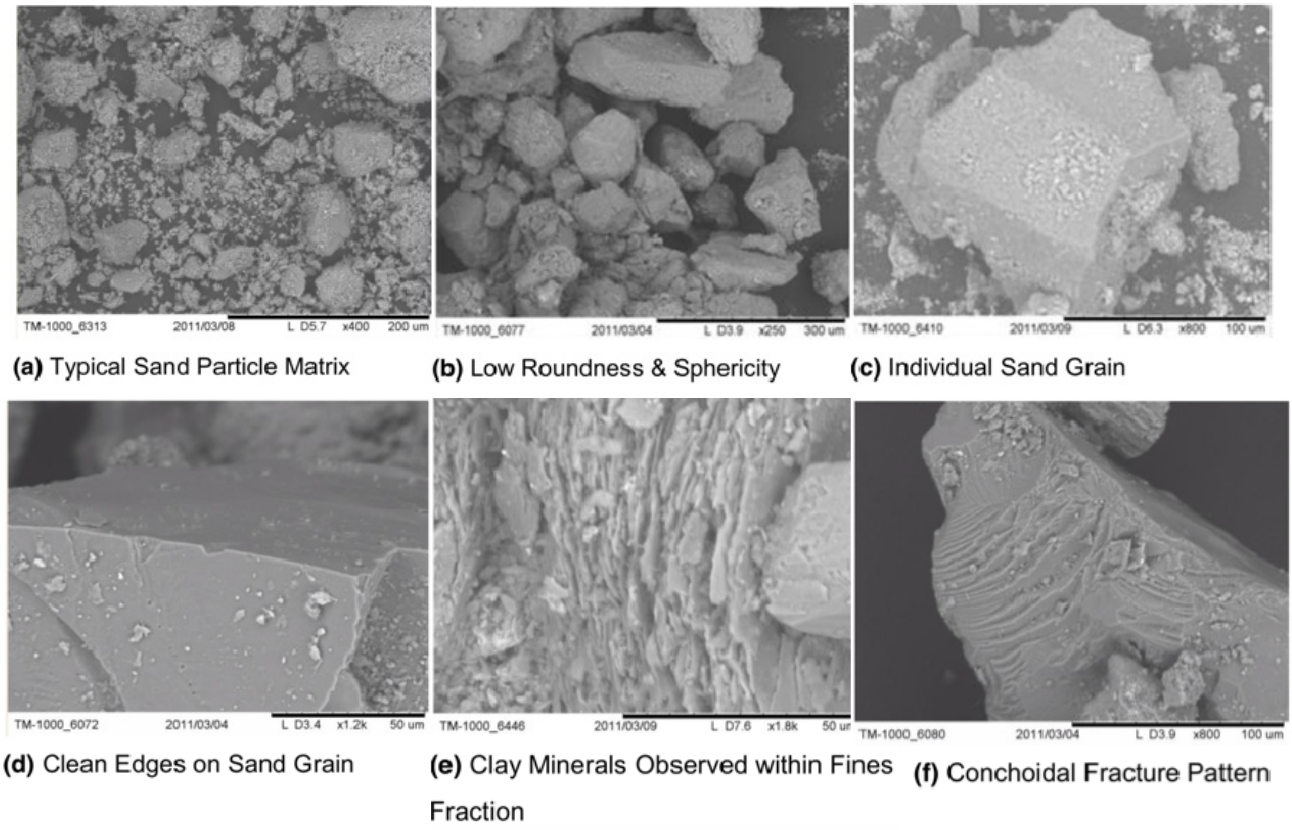

Figure 7. Images of Blessington sand samples under a SEM (after [9]).

Particle roundness and sphericity were determined using ImageJ software [16] along with the plugin called Particle8_Plus [17]. The software calculates the roundness (R) and sphericity (S) of particles using the following formulae:

$$S = R_{ic}/R_c \tag{1}$$

$$R = 4A_c/\pi L^2{}_{major} \tag{2}$$

where: R_{ic} is the radius of the largest inscribed circle, R_c is the radius of the circumscribed circle centred at the particles centre of mass, A_c is the cross-sectional area of the particle and $L^2{}_{major}$ is the length of the particles major axis. Figure 8 shows the average roundness and sphericity values with depth of the borehole samples. Both the sphericity and roundness are shown to be relatively constant with depth. The sphericity ranges between 0.45–0.54 and roundness ranges between 0.55–0.63 [9].

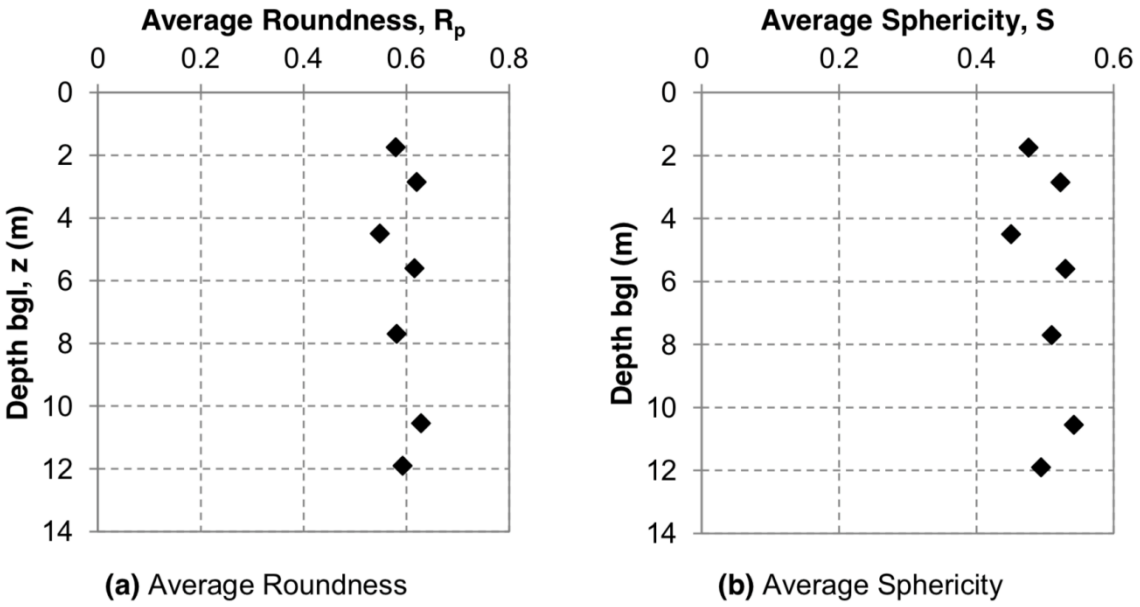

Figure 8. Borehole Samples Shape Parameters at Different Sampling Depths (after [9]).

7. In-situ testing

7.1. CPT testing

A total of 15 CPT tests have been performed in the upper-site and 10 CPT tests in the lower site by InSitu Ground Investigation Ltd. The CPT tests were performed to depths of more than 10 m across the two sites in order to inform future pile load tests. Profiles of the max, min and mean CPT cone resistance for the upper- and lower-sites are shown in Figure 9. The CPT profiles from the lower-site exhibit notably higher cone resistance over the top 2 m, as a result of higher levels of over-consolidation due to the removal of at least 15 m of sand through quarrying. Below 2 m depth, the profiles show broadly similar q_c values, although the upper-site profile increases with depth compared with the lower-site profile which is relatively constant with depth. Both sites show highly consistent q_c values across each site, indicating little lateral special variability. The variability in CPT cone resistance increases below 8m depth in the lower-site.

7.2. Dilatometer Testing

Dilatometer tests were undertaken at both the upper- and lower-sites. The testing involved pushing a blade cell into the deposit and undertaking a lateral expansion of the cell face (comprised of a flexible membrane) to a displacement of 1.1mm at regular depth intervals of 0.25 m. The initial expansion pressure (the lift-off pressure p_0) and final strain level pressure (the limit pressure, P_L) were recorded (Figure 10). The dilatometer tests were terminated at 6 m depth due to the 20 t reaction force available from the CPT truck being exceeded. The lift-off pressure, P_0, increased with depth from 500 kPa at shallow soundings to greater than 1000 kPa at 6 m depth. The limit pressure showed similar increases with depth from 2 MPa at 0.5 m depth to 4 MPa at 6 m depth. The high lateral pressures

required to expand the cell at such shallow depths is indicative of high lateral earth pressures resulting from past over-consolidation [9].

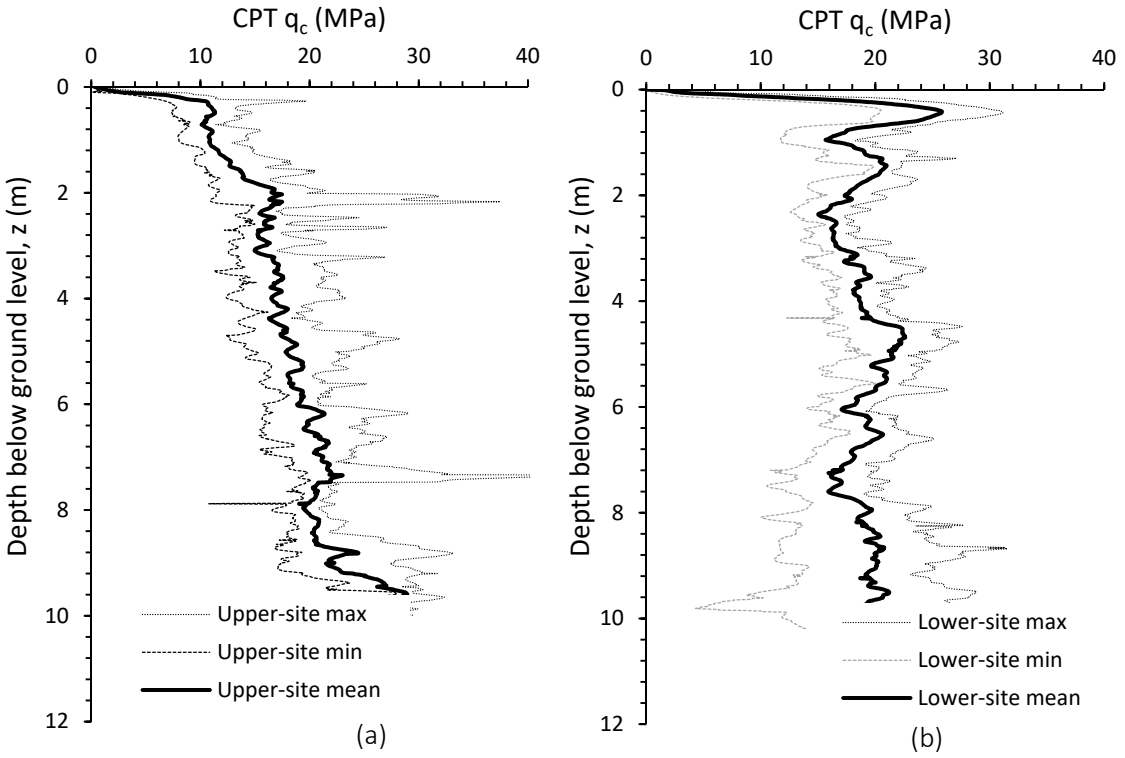

Figure 9. Summary of CPT cone resistance from a) upper-site and b) lower-site.

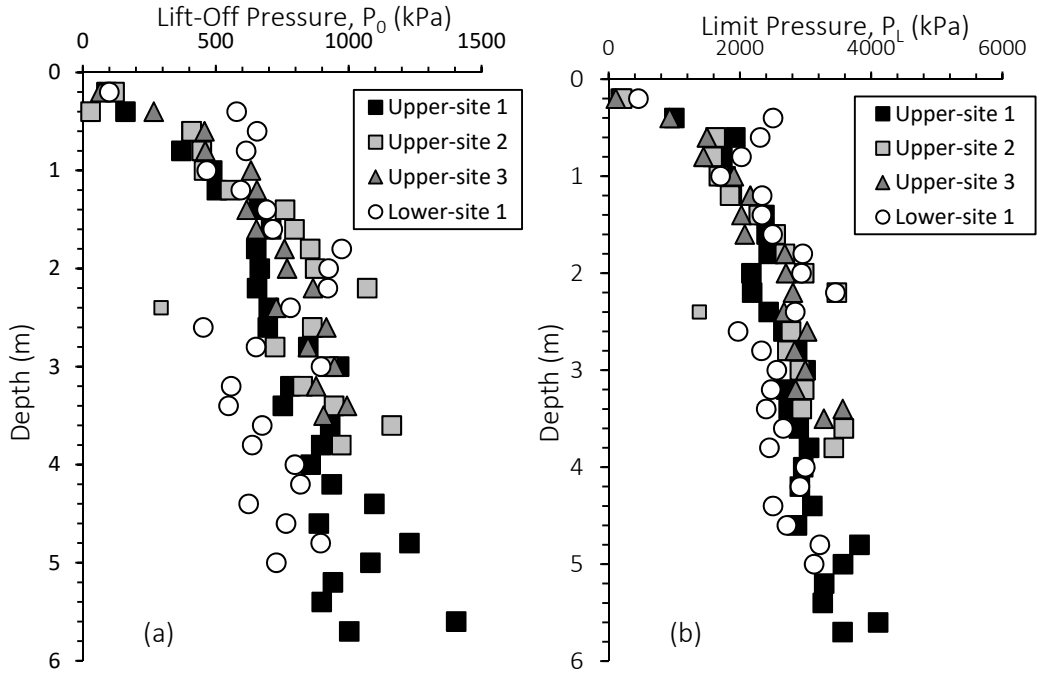

Figure 10. Dilatometer a) Lift-off pressures and b) Limit pressures from Blessington.

8. Over-Consolidation Ratio

8.1. Oedemeter testing

Oedometer testing was undertaken on samples recovered from the sonic cores from the upper-site between depths of 1.75 m and 14 m. Based on the Casagrande method the pre-consolidation stress was estimated to vary between 600–1000 kPa [9]. The OCR was shown to vary from ~15 at 1.75 m depth to less than 5 at 5 m depth (Figure 11a).

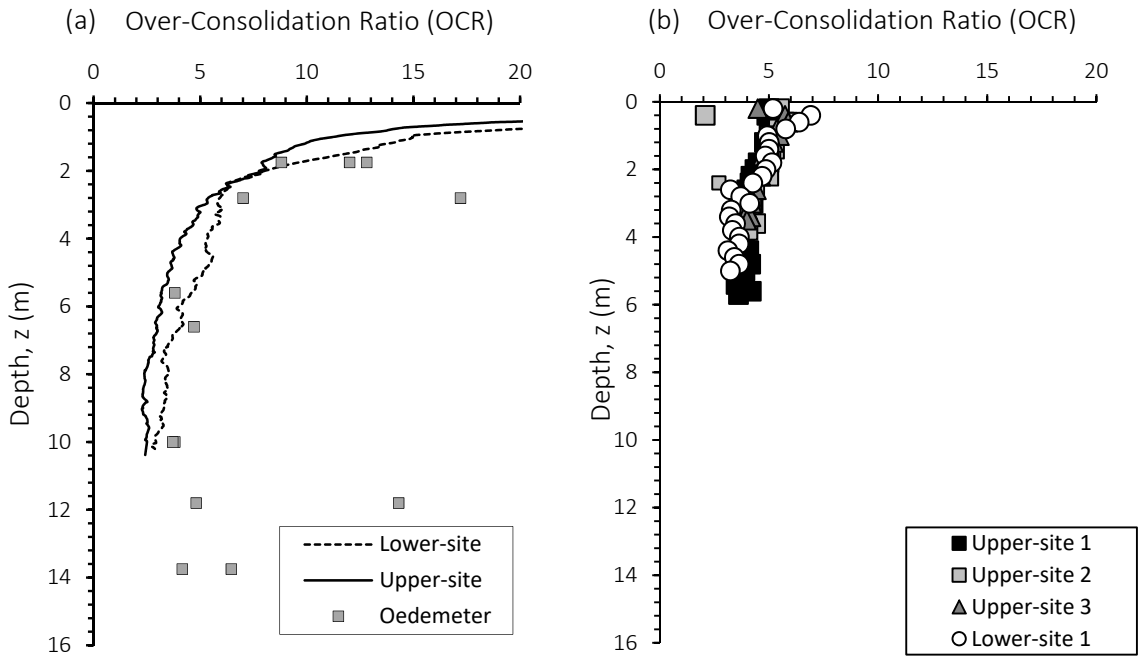

Figure 11. OCR from a) Oedometer and CPT tests and b) Dilatometer tests.

8.2. CPT correlations

CPT correlations were also used to derive the OCR using the equations suggested by [18]:

$$OCR = \left[\frac{1.33 * {q_t}^{0.22}}{K_{0NC} * {\sigma'_{vo}}^{0.31}}\right]^{\frac{1}{\alpha-0.27}} \quad (3)$$

The value of α in equation was taken as $sin\varphi_{cv}$. The CPT correlation generally shows very good agreement with the Oedometer test data as seen in Figure 11a.

8.3. Dilatometer correlations

Correlations with the OCR from dilatometer lift-off pressure, P_0, have been proposed by Marchetti [19]:

$$OCR = 1.6454ln(K_D) - 0.3693 \quad (4)$$

where: $K_D = (P_0 - u_0)/\sigma'_{v0}$.

The estimations of OCR using the above correlations are shown in Figure 11b. The estimated OCR values from the dilatometer testing are significantly lower than both the Oedometer and CPT correlations for the top 3 m but are in reasonable agreement below 3 m depth.

9. Friction angle

9.1. Shear box testing

A suite of Constant Normal Load (CNL) shear box testing was undertaken on reconstituted Blessington sand from the upper-site at normal stress levels ranging from 50 to 250 kPa [20]. Results from the tests are provided in Figure 12. After initially contracting the samples exhibit strong dilation, with larger dilation noted at lower stress levels. The peak friction angle mobilized reduced from 57° to 42° as the normal stress increased from 50 to 250 kPa. The residual friction angle mobilized was 37°.

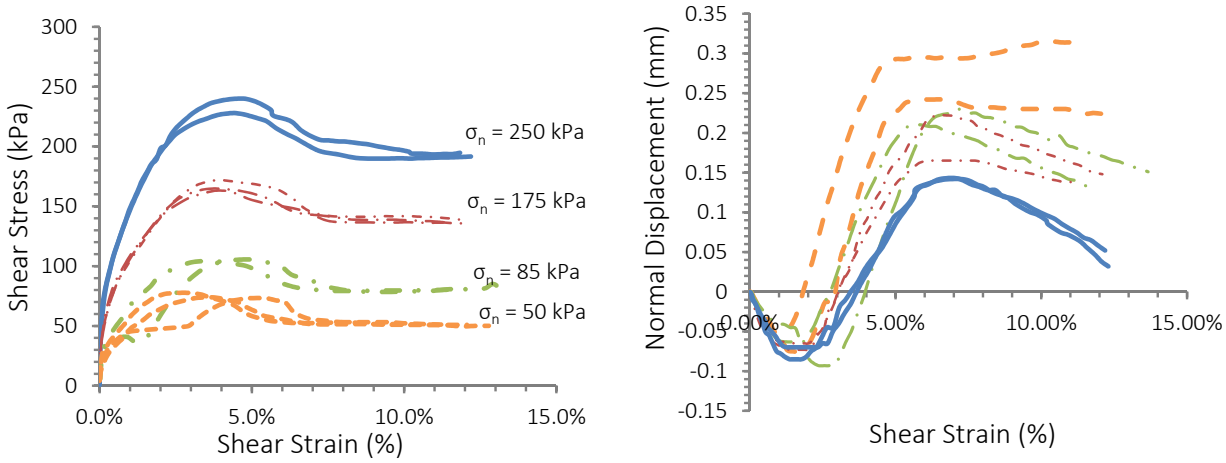

Figure 12. Direct Shear test results from Blessington upper-site (after [20]).

9.2. Triaxial testing

Compression triaxial testing on reconstituted samples of Blessington sand prepared at a relative density ≈100% (according to BS1377) were reported by Tolooiyan and Gavin [21] for the upper-site. The reconstituted samples were formed using the procedure described by Tolooiyan and Gavin [21]. In this method a PVC cylinder (with a diameter of 50 mm and length 100 mm), which was lubricated on the inside surface, was filled with sand at the natural moisture content. The sample which was compacted into layers using a vibrating hammer was then placed in a modified oedometer cell. A vertical pressure of 800 kPa was then applied for a period of days. A constant volume friction angle of 37° was measured with peak values ranging from 54 to 42 degrees, decreasing with increasing stress level [9]. A plot of the normalized stress-strain curves from three of the tests are shown in Figure 13.

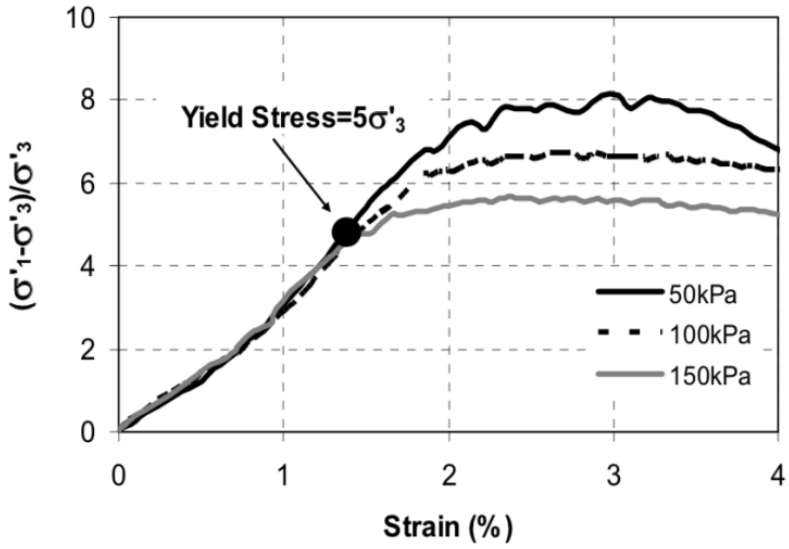

Figure 13. Triaxial test results from Blessington upper-site (after [21]).

9.3. Correlations with in-situ testing

Estimates of the peak friction angle were calculated using the formula suggested by [22] for triaxial strain conditions:

$$\varphi'_p = \varphi'_{cv} + 3(D_r(10 - \ln p') - 1) \tag{5}$$

where D_r is the relative density of the sand and p' is the mean effective stress. The value of p' was derived using the K_0 formula proposed by Kulhawy and Mayne [23] where $K_0 = (1 - sin\varphi).OCR^{sin\varphi}$. The relative density was calculated from the CPT cone resistance as follows [17]:

$$D_r = \sqrt{\frac{Q_{tn}}{305 \cdot OCR^{0.15}}} \tag{6}$$

where Q_{tn} is the normalized cone resistance taken as $Q_{tn} = \left(\frac{q_t - \sigma_{v0}}{p_a}\right) \cdot \left(\frac{p_{ref}}{\sigma'_{v0}}\right)^n$ and n is the stress exponent which varies between 0 and 1 depending on soil type and stress level. The value for n was solved iteratively until the convergence tolerance was reached using the method proposed by [24]. Values of the peak friction angle and relative density estimated from CPT are plotted against lab test results in Figure 14. At shallow depths (below 6 m) the CPT correlation tends to predict lower values of peak friction angle compared with those derived from the direct shear and triaxial tests. This may be due to the difference in relative density between in-situ conditions and the reconstituted laboratory samples. Below 6 m depth there is good agreement between the lab tests and CPT correlations.

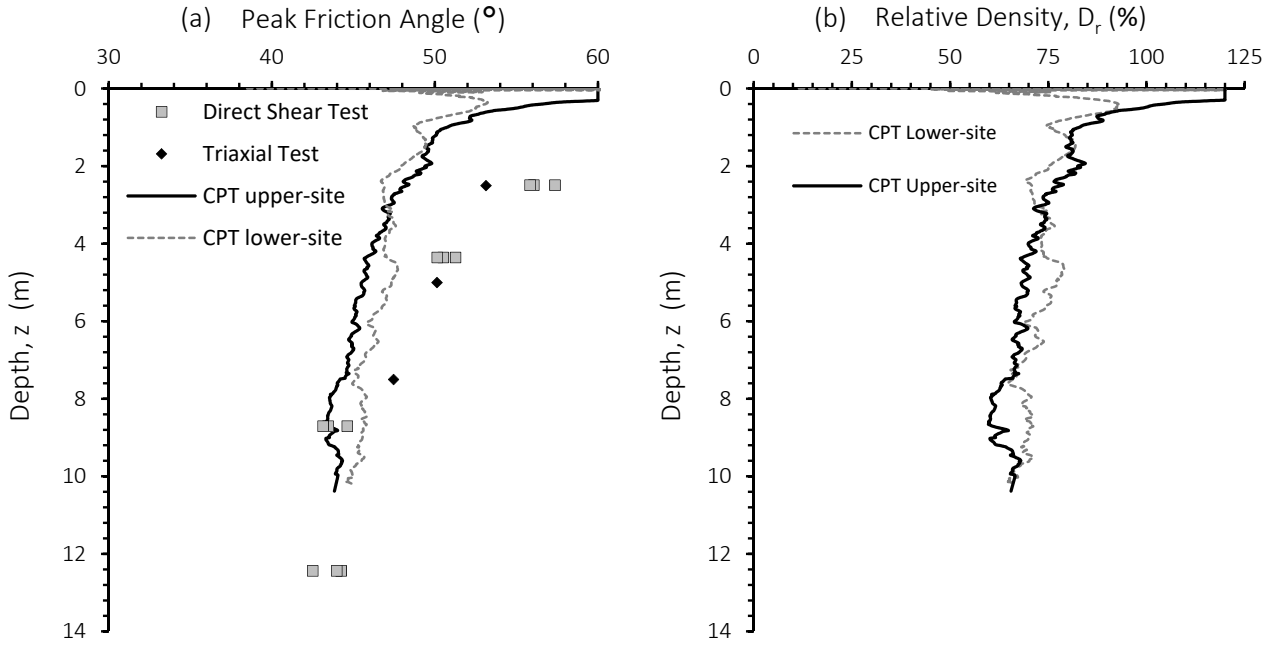

Figure 14. a) Peak Friction Angle and b) Relative Density at Blessington.

10. Shear modulus

The small strain shear modulus from the upper site was established from shear waves velocities established from Spectral Analysis of Surface Waves (SASW) and Multi-channel Analysis of Surface Waves (MASW). Profiles of the shear modulus with depth are provided in Figure 13 and shows the small strain shear modulus increasing from approximately 70 MPa at 1m depth to 200 MPa at 10 m depth. The G_0 profile was also estimated from CPT correlations by Schnaid and Yu [25] (Eq 7):

$$G_0 = \alpha \cdot \sqrt[3]{\sigma'_{v0} \cdot q_c \cdot P_a} \tag{7}$$

The value of α is typically in the range between 110 and 280 for un-cemented sands. The G_0 profile estimated from CPT using α = 250 is plotted in Figure 15 and matches very closely the G_0 profile derived from shear wave velocity measurements.

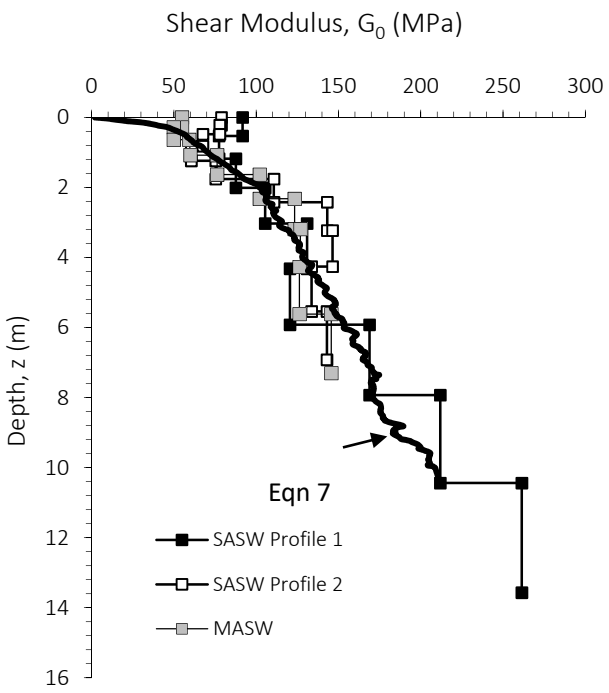

Figure 15. Small Strain Shear Modulus profiles from Blessington upper-site.

11. Combining field and lab tests to investigate ageing

A large number of the field tests performed at the Blessington test site relate to research into pile ageing. This is the phenomenon whereby the axial shaft capacity of driven pile in sand is seen to increase substantially over the weeks and months following pile driving. A summary of the results from a suite of tension static load tests performed on 340 mm diameter open-ended driven piles is shown in Figure 16. The pile tension capacity was seen to increase more than three-fold over a period of 100 days following installation and generally displayed rates of increase that were comparable to those observed in similar field tests performed by workers at Imperial College and Norwegian Geotechnical Institute [26]. One pile (S4) tested on day 30 exhibited a comparably low axial capacity [27]. The plugging and driving response of pile S4 was similar to all other piles installed up to the final 1 m of penetration. Thereafter, the Incremental Filling Ratio (IFR) increased and the number of blow-counts needed to drive the pile reduced when compared to the other piles installed the same day (S2, S3 & S5) suggesting that the unusually low capacity of pile S4 was influenced by the local variability in the soil profile that led to much reduced plugging and reduced installation resistance for the last 1m of pile installation (between 6 m and 7 m bgl).

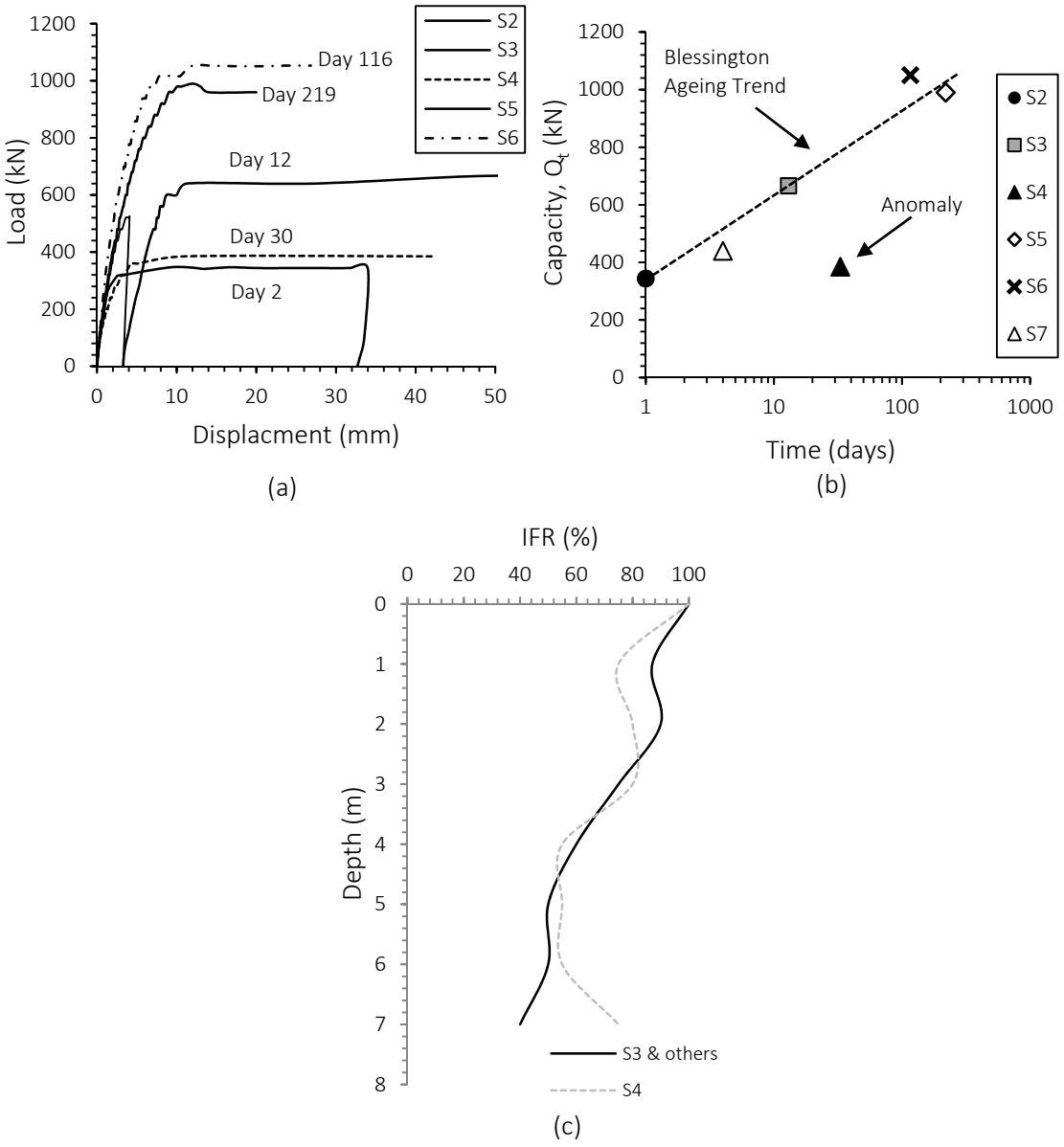

Figure 16. Pile Ageing test results from Blessington (a) Load-displacement, (b) Increase of capacity with time (c) IFR values during installation.

Gavin et al. [4] reported that the primary mechanism contributing to the large capacity gains at Blessington was increased dilation at the pile-soil interface with time. The role of creep in this process is discussed in Gavin et al. [26]. The zone where enhanced dilation contributed to large shear stress increase at Blessington was confined to the lower pile shaft where mean stress levels induced by driving were largest. To investigate the influence of time on stress-strain response a series of Constant Normal Load, CNL interface direct shear tests were recently performed on Blessington sand samples using a mild steel interface (Figure 17). The samples were prepared to a relative density of ~70%, with a moisture content of ~15% and tested initially at normal stresses of 150 and 350 kPa (dashed lines). The interface was initially smooth as a result of machining, with an average surface roughness, R_a, of 2.8 μm (measured using a mechanical profilometer). The samples were then sheared forward and backward in the shear-box for 5 cycles (to represent pile installation shearing cycles) before being allowed to age under the applied normal stress for 21 days. Following the ageing period the samples

were sheared again. The aged samples showed a significant increase in dilation and peak shear stresses compared with their original state (solid lines in Figure 17). Once the aged tests were completed, the interfaces were removed and showed signs of heavy rusting with sand particles bonded to the mild steel resulting in a much rougher interface. Similar adhesion of soil particles to the test piles were reported in Gavin et al. [4]. Profilometer measurements of the aged interface after testing indicated an average surface roughness, R_a, of 29.4 μm, a ten-fold increase on the original average roughness. Interestingly, follow on tests, with no installation cycles performed, did not exhibit the same large increases in dilation after ageing.

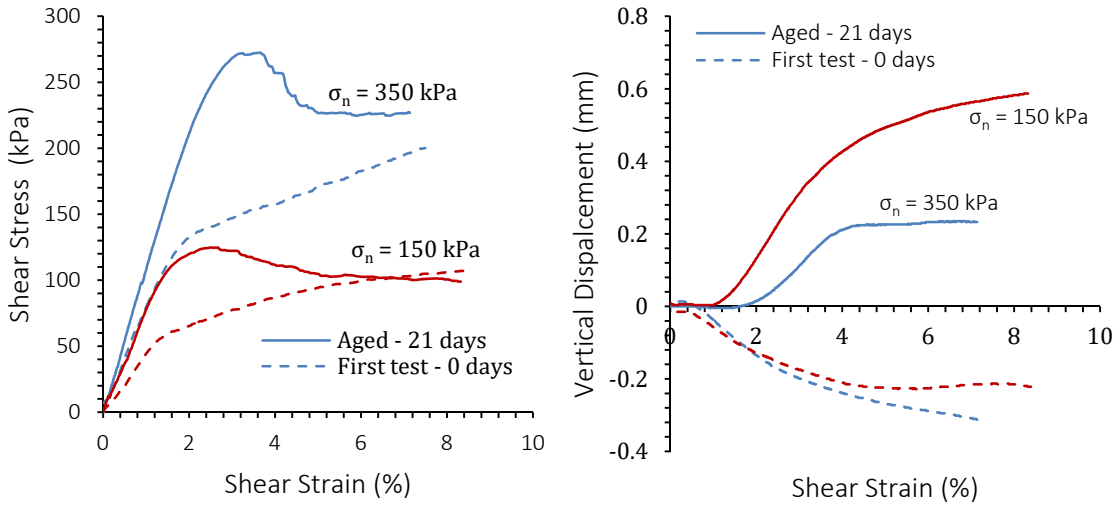

Figure 17. Interface CNL shear box tests on aged and unaged soil samples.

12. Conclusions

The paper provides an overview of the geotechnical characterisation of the Blessington dense over-consolidated sand site where a number of field tests investigating foundation systems have been performed. The paper focusses on the strength and stiffness parameters measured from in-situ tests, considers the accuracy of common correlations for transforming in-situ test data to strength and stiffness values and finally shows how combined field tests using instrumented piles and element testing in the laboratory provides insights into ageing effects on steel axially loaded displacement piles. Key insights from the reported work are:

1. Although it has a relatively complex geological history, the test site is relatively uniform with low vertical and horizontal variability of both strength and laboratory stiffness properties. The in-situ test profiles at two locations, an upper site and lower site were comparable. Despite the upper-site being a partially saturated deposit and the lower site having the water table within 2 m of ground level. Differences in the near-surface CPT values are most likely related to the difference in the time of exposure since excavation.
2. Blessington sand is seen to have a high constant volume friction angle of 37°. The material dilates strongly at low stress levels with peak friction angles as large as 54° being recorded.

3. Even in this relatively uniform deposit, ageing tests on four identical piles revealed one anomalously low capacity. The role of natural variations in the CPT q_c value in influencing the plugging response and therefore capacity was very important.
4. In direct interface shear tests which included large deformation phases to model pile installation, followed by ageing tests, the material response transformed from contractive response for immediate tests, to highly dilative response when the samples were allowed to age for twenty-one days.

Acknowledgments

The test authors would like to thank Roadstone Ltd. for permission to use the Redbog Quarry. The authors would like to acknowledge the financial support of Science Foundation Ireland and Mainstream Renewable Power. The test site has been used by many former students at University College Dublin and we acknowledge the contributions of Lisa Kirwan, Paul Doherty, David Cadogan, Gerry Murphy, Irfan Chatta, Shane Donohue and Ayman Abelgawa.

Conflict of interest

The author declares that there is no conflict of interest associated with this research.

References

1. Igoe D, Gavin K, O'Kelly B (2010) Field tests using an instrumented model pipe pile in sand. *Physical Modelling in Geotechnics—Proceedings of the 7th International Conference on Physical Modelling in Geotechnics 2010, ICPMG*.
2. Igoe D, Doherty P, Gavin K (2010) The development and testing of an instrumented open-ended model pile. *Geotech Test J* 33: 72–82.
3. Igoe D, Gavin K, O'Kelly B (2013) An investigation into the use of push-in pile foundations by the offshore wind sector. *Int J Environ Stud* 70: 777–791.
4. Gavin KG, Igoe D, Kirwan L (2013) The effect of ageing on the axial capacity of piles in sand. *Proc Inst Civ Eng Geotech Eng* 166: 122–130.
5. Igoe D, Gavin K, Kirwan L (2013) Investigation into the factors affecting the shaft resistance of driven piles in sands. In: *Installation Effects in Geotechnical Engineering—Proceedings of the International Conference on Installation Effects in Geotechnical Engineering, ICIEGE 2013*.
6. Murphy G, Igoe D, Doherty P (2018) Gavin KG. 3D FEM approach for laterally loaded monopile design. *Comput Geotech* 100: 76–83.
7. Igoe D, Gavin KG, O'Kelly BC (2011) Shaft Capacity of Open-Ended Piles in Sand. *J Geotech Geoenvironmental Eng* 137: 903–913.
8. Doherty P, Igoe D (2013) A Driveability Study of Precast Concrete Piles in Dense Sand. *DFI J J Deep Found Inst* 7: 3–16.
9. Doherty P, Kirwan L, Gavin KG, et al. (2012) Soil Properties at the UCD Geotechnical Research Site at Blessington. In: *Bridge and Concrete Research in Ireland*, Dublin.
10. Syge FM, West Wicklow (1977) In: South-East Ireland. In: Int Union of Quartenary Research Fieldguide.

11. Cohen JM (1979) Deltaic sedimentation in glacial lake in Blessington in County Wicklow. *Moraines Varves*, 357–367.
12. Cohen JM (1980) Aspects of glacial lake sedimentation. Trinity College Dublin.
13. Philcox ME (2000) The glacio-lacustrine delta complex at Blessington, Co. Wicklow and related outflow features. In: *Guidebook of the 20th Regional Meeting of Sedimentology*, Dublin: IAS Special Publication, 129–152.
14. Coxon P (1993) Irish Pleistocene biostratigraphy. *Irish J Earth Sci* 12: 83–105.
15. Kirwan L (2014) Investigation into Ageing Mechanisms for Axially Loaded Piles Driven in Sand. University College Dublin.
16. Rasband WS (2004) ImageJ. Bethesda, MD: National Institutes of Health.
17. Landini G (2006) Particle8_Plus plugin in ImageJ.
18. Mayne PW (2001) Stress-strain-strength-flow parameters from enhanced in-situ tests. In: *Proceedings International Conference on In-Situ Measurement of Soil Properties & Case Histories, Bali*, Indonesia, 27–48.
19. Marchetti S, Monaco P, Calabrese M, et al. (2006) Comparison of moduli determined by DMT and back figured from local strain measurements under a 40 m diameter circular test load in the Venice area. *Proc From the second international flat dilatometer conference*.
20. Spagnoli G, Doherty P, Wu D, et al. (2015) Some mineralogical and geotechnical properties of carbonate and silica sands in relation to a novel mixed-in-place pile, *12th Offshore Mediterranean Conference and Exhibition*, Italy: Ravenna.
21. Tolooiyan A and Gavin (2011) Modelling the Cone Penetration Test in sand using Cavity Expansion and Arbitrary Lagrangian Eulerian Finite Element, Computers and Geotechnics, Vol. 38, pp 482-490.
22. Bolton MD (1986) The strength and dilatancy of sands. *Géotechnique* 36: 65–78.
23. Kulhawy FH, Mayne PW (1990) Manual on estimating soil properties for foundation design.
24. Robertson PK, Cabal K (2014) Guide to cone penetration testing for geotechnical engineering—6th Edition.
25. Schnaid F, Yu HS (2007) Interpretation of the seismic cone test in granular soils. *Géotechnique* 57: 265–272.
26. Gavin K, Jardine RJ, Karlsrud K, et al. (2015) The effects of pile ageing on the shaft capacity of offshore piles in sand. *International Symposium Frontiers in Offshore Geotechnics (ISFOG),* London: Taylor & Francis, 129–151.
27. Gavin K, Igoe D (2019) A Field Investigation into the Mechanisms of Pile Ageing in Sand, Submitted to *Geotechnique*.

AIMS Press